

A HIGH-RESOLUTION PHOSPHOR SCREEN BEAM PROFILE MONITOR*

S. Yencho and D.R. Walz

*Stanford Linear Accelerator Center
Stanford University, Stanford, California, 94305*

Abstract

A high-resolution luminescent screen beam profile monitor was developed to allow viewing of both conventional large diameter SLAC e^+/e^- beams, and also collider rf-bunches having small transverse spatial extent, with one instrument. The principal features of the monitor are described. They include the two-power magnification system offering magnifications of 12 and 78X, respectively; the reticle grid which is optically superimposed on the screen image by a cube beam splitter; selection of a suitable camera; and the $Al_2O_3(Cr)$ phosphor screen. A simplified version of the monitor for viewing of only micron-sized beams for applications in the collider arcs and final focus regions and achieving a magnification of $\sim 40X$, coupled with a resolution of $\sim 20\mu m$ is also presented.

1. Introduction

The transverse spatial extent of the positron and electron bunches in the Stanford Linear Collider (SLC) is expected to vary from several tens to hundreds of microns (μm) in the special insertion matching sections of the collider arcs and the final focus region. It is highly desirable to monitor, at least intermittently, the transverse profile, position and emittance of these micronsized beams in various locations of the SLC. Deviations from the norm in any of these parameters almost always result in emittance growth at the interaction point, and thus, loss of luminosity. An intercepting luminescent phosphor screen, while destructive in nature, can be a valuable complement to other non-destructive methods of beam monitoring if appropriately designed, and used intermittently. One area where beam diagnostics is especially important is in the linac-to-arcs matching sections in the front end of the beam switchyard, i.e. after completion of acceleration and before beam insertion into the arc lattice. Since this is a region where both conventional SLAC beams with large transverse dimensions as well as micronsized SLC beams can be transported, it appeared desirable to develop a beam profile monitor capable of satisfying both conditions with one instrument. Important design criteria were the dual magnification feature, compactness in beam axial direction, moderate radiation hardness, high reliability due to limited accessibility and convertibility of the basic design to a single high-magnification instrument for use in other areas of the collider where only SLC-beams need to be monitored.

2. Evolution of Design Concepts

Several concepts were explored in depth before the final design evolved. One of these included a two-camera system, one for low power, and the other for high-power magnification. This approach proved to be costly due to elaborate hardware needs with questionable reliability in the radiation environment; it was abandoned in favor of a single camera design.

The angle between the beam intercepting target screen and the beam, as well as that between the screen and the optical axis of the camera, received special scrutiny. Traditionally, a 45° angle had been used. This was a good compromise, and it offered sufficient depth of field for the low-power magnification optics needed to view millimeter- or centimeter-sized beams. It was highly desirable for the new monitor to produce an image which could be viewed in correct perspective on a CRT monitor. A 45° target image would have to be reduced along one axis by a factor of 1.414 for this to become reality. On the other hand, a 30° target angle would require a reduction of only 1.155 which could be accomplished by decreasing the scan height on existing monitors without the need for specialized hardware. Viewing the target at 90° was a must for high-power magnification and resultant small depth of field.

Another concept which received scrutiny was the placement of fiducials on the screen. Traditionally, such features, as well as identifying letters and numbers, were drawn, painted, silk-screened or otherwise applied directly onto the screen. In some cases, a mask overlay was added, or fine wires stretched over the screen and located by means of an array of precisely drilled, small diameter holes. Since micronsized beams can easily be hidden behind such fiducials, it was decided early on to try and optically superimpose the fiducials and match them to the desired magnification. This can be accomplished via a cube beam splitter described in more detail below.

The selection of an appropriate TV camera also received specific attention. The radiation environment in the beam switchyard calls for radiation hard cameras. They are very expensive, and past experience at SLAC showed that inexpensive non-radiation hardened vidicon-tube type cameras present a good economical solution, even though they need to be replaced more often than hardened cameras. The decision was made to use an inexpensive camera and to design for easy replacement. A vidicon-tube (RCA-TC2511) was selected over an Ultricon or Saticon type tube because of its excellent resolution, good contrast and low light capability.

3. The Monitor Design

The final design is comprised of a TV camera, one lens, a cube beam splitter, a reticle grid, and the movable phosphor screen mounted in a vacuum chamber. The basic optical arrangement is shown in Fig. 1. The key to this scheme is the movable lens which can be translated between two different foci. It, thus, provides the dual magnification feature for imaging either a large or a small target onto the vidicon tube. In both cases, the exposed area of the vidicon tube is constant. Since the lens is to perform both effective magnifications and reductions of flat fields of view, an enlarging lens with symmetrical optics was desirable. A Nikon 135mm f/5.6 enlarging lens was chosen because of good resolution, small size, and

* Work supported by the Department of Energy, contract DE - AC03 - 76SF00515.

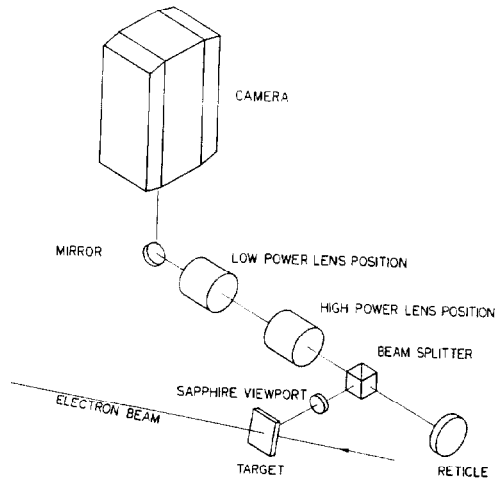


Fig. 1 - - Optical Arrangement of Profile Monitor

moderate cost. This focal length was selected, because, in the high-power configuration, it yielded an optimal value of the modulation transfer function (MTF), and provided the desired field of view. It also achieved the desired resolution for both the low- and high-power magnification positions.

The total depth of field is given by $D_{tot} = D_1 + D_2$, where D_1 and D_2 are the depth of the far and near field, respectively. Utilizing the basic optical relationships, $F = sM(M+1)$, where F is the effective focal length of the lens, s is the distance from the lens to the point in focus, and M is the lens magnification; and if c is the circle of finest resolution and f is the f-stop of the lens, then the following expression can be written:

$$D_1 = \frac{s}{1 + scf/F^2} \quad , \quad D_2 = \frac{s}{1 - scf/F^2}$$

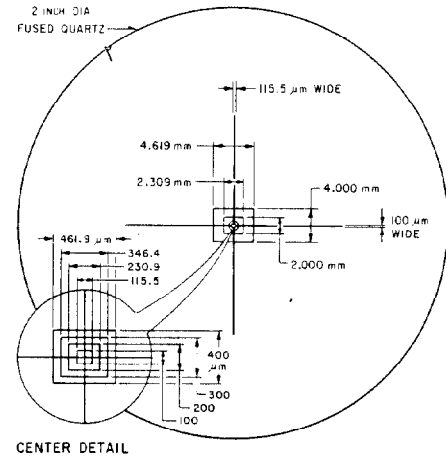
After combining and simplifying, the equation for the total depth of focus becomes:

$$D_{tot} = \frac{2(M+1)F^5M}{M^2F^4 - F^2(M+1)^2c^2f^2}$$

Solving for c will readily yield the resolution of the system.

The lens has to shuttle between the high- and low-power positions. This is accomplished by means of precision-ground steel rods and recirculating ball bushings, which ensures accuracy and low friction. Since the lens moves only between two fixed positions an air cylinder was chosen as prime mover over more expensive stepping motor/lead screw combinations.

A reticle was designed, as shown in Fig. 2, to be superimposed over the target image. This reticle consists of chromium lines of varying widths evaporated onto a quartz disc. The rectangles on the reticle will project as squares when the reticle is tilted at 30° . Therefore, after superposition of the reticle onto the target via a cube beam splitter, the combined image has both the x and y axes scaled appropriately. To compensate for manufacturing tolerances the reticle is mounted in an assembly which allows adjustment of x and y positions, as well as the angle in the z -plane.

Fig. 2 - - Reticle Design
Two-Power Magnification

Two mirrors are used in the system (one in the x -plane, the other in the y -plane) to re-orient the image before it reaches the vidicon pick-up tube so that the image appears in its correct orientation on the CRT monitor.

One of the most crucial parameters in determining the system resolution was the lens-to-target distance. It must be minimized to guarantee accuracy. A special viewport was needed between the beam splitter and the target to reduce this distance. A 3mm-thick sapphire window brazed into a covar re-entry port was used to hold the deflection due to the vacuum load to less than $1/4$ wavelength of mercury light. The whole assembly was mounted to a rigid base plate to assure dimensional stability and keep the optical components aligned when in service. The complete monitor assembly is shown in Fig. 3.

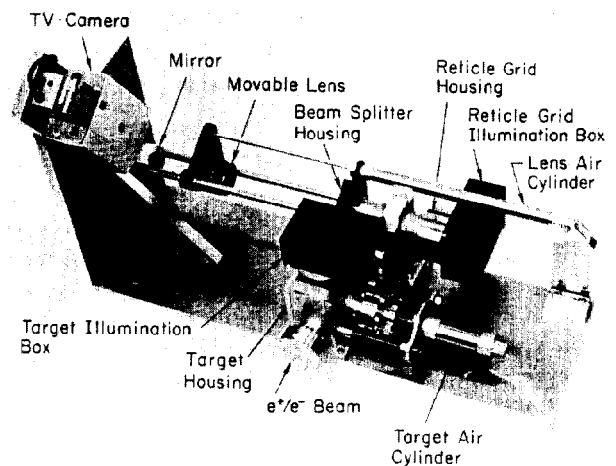


Fig. 3 - - Profile Monitor Assembly

4. The Phosphor Screen

The target material chosen is a chromium-activated Al_2O_3 phosphor screen produced by appropriately anodizing a $1/2$ mm thick aluminum plate. It is an improved SLAC version of a scintillator screen originally developed elsewhere.⁴

This material is highly radiation resistant, and numerous such screens were used at SLAC during the past 12 years. Other phosphors which are commercially available in powder form, and which need to be either sprayed or floated with a vehicle onto a support screen, have poor adhesion, and make fragile targets. $\text{Al}_2\text{O}_3(\text{Cr})$, having been generated on the support foil, has excellent adhesion, and makes a rugged target.

The light output is in the red part of the spectrum ($\lambda \sim 693 \text{ nm}$, Cr^{3+} excitation lines), and is therefore not perfectly matched to the spectral response of the Vidicon peaked at $\sim 530 \text{ nm}$. Furthermore, the response to electron beam intensity is linear over a wide range of currents. The 1/2mm plates are typically oxidized to $\sim 60\%$ of their thickness. The sensitivity of the best screens was measured to be $\sim 1 \times 10^9 \text{ e}^-/(\text{cm}^2 \text{ sec})$. This guarantees more than adequate light output for all envisioned collider applications.

One of the limits on resolution is dictated by the granularity of the screen material. The Al_2O_3 film exhibits a rough, sandpaper-like surface. Typical "grain" sizes measured were 50 to $100 \mu\text{m}$. Another limit is placed on the overall performance of the monitor by the temperature rise per bunch in the aluminum backing. For the expected collider single bunch intensity of $5 \times 10^{10} \text{ e}^+/\text{e}^-$, having gaussian distribution with $\sigma_b = 25 \mu\text{m}$, and normally incident on an aluminum foil ($T_{\text{melt}} = 659^\circ\text{C}$), the temperature rise is $\sim 525^\circ\text{C}/\text{bunch}$. Rotation of the screen relative to the incident beam direction reduces this value, but $\sigma_b \sim 20 \mu\text{m}$ is probably as small as can be tolerated for long-term exposure.

The screen is remotely inserted into, and removed from, the passage of the beam by a means of a second air cylinder.

5. Performance Specifications

A final test of the optical components was performed. After set-up, the optical apparatus was fine-tuned to maximize the resolution and image clarity. An optical resolution target was focused upon, and a video analyzer attached to the camera. The amplitude of various sets of images on the target was measured on an oscilloscope. From this data, the system MTF curve, shown in Fig. 4, was plotted. This curve defines the capabilities of the system for different object sizes which are likely to be encountered in service. The following specifications further define the system's performance capabilities:

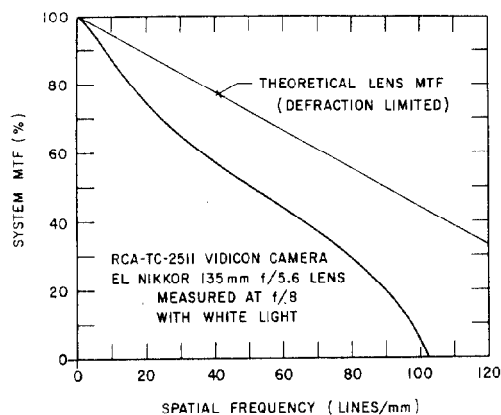


Fig. 4 -- High-Power Modulation Transfer Function

	High Power	Low Power
Limiting Resolution	$9.7 \mu\text{m}$ (2.5 TV-lines)	$40 \mu\text{m}$ (1.7 TV-lines)
System Magnification (12" Monitor)	78X	12X
Field of View	3.61mm	22.6mm

Overall, 700 TV lines define the monitor image. The e^+/e^- beam images to be viewed are large enough to clearly show beam shape and dispersion. The field widths are also large enough to capture the beam if it has significantly deviated from the nominal trajectory to which the monitor was aligned.

6. One Power Magnification Monitor

Luminescent screen monitors are also contemplated for some locations in the SLC arcs matching sections, and some regions of the final focus system. There, the need is for monitoring profile, emittance and position of only micronsized collider beams, and a simplified version of the instrument described above, offering only single magnification, will suffice. The assumed smallest transverse beam size to be monitored was $2\sigma_b = 60 \mu\text{m}$, and average size $2\sigma_b \sim 100 \mu\text{m}$. The total beam stay clear region in these sections is $\geq 1 \text{ cm}$.

A good compromise between performance and cost was found for a combination of the RCA-TC2511 camera with vidicon tube, and a Schneider 80mm f/5.6 Componon-S enlarging lens. This combination was found to be \sim one-half the cost of the next best solution, and has a favorable MTF. The distance from the screen [$\text{Al}_2\text{O}_3(\text{Cr})$] to the vidicon tube is 31.5 cm. The lens is fixed, and a reticle is, again, superimposed onto the target image by a cube beam splitter, as described above. The target is also rotated by 30° relative to the trajectory of the beam to be monitored. The following is a set of performance specifications: Limiting resolution $\sim 30 \mu\text{m}$ (8 TV lines; 13 TV lines for $100 \mu\text{m}$); system magnification $\sim 39\text{X}$ (14 inch diagonal monitor); field of view 7.3mm; optical distances $U = 16.23 \text{ cm}$, and $V = 15.78 \text{ cm}$; image size 2.34mm for $60 \mu\text{m}$ object, and 3.9mm for $100 \mu\text{m}$ object. The above are calculated values, and no prototype has been built yet.

Acknowledgements

A debt of gratitude is owed to F. Plunder, M. Ross, P. Shapiro, F. Stiver and B. Sukiennicki for their valuable contributions to this project, and also to K. Fraser, who prepared this manuscript.

References

- [1] E.H. Linfoot, *Fourier Methods in Optical Image Evaluation*. New York: Focal Press, 1964.
- [2] J.W. Goodman, *Introduction to Fourier Optics*. New York: McGraw-Hill, 1968.
- [3] R.R. Shannon, J.C. Wyant Eds., *Applied Optics and Optical Engineering*. New York: Academic Press, 1980.
- [4] R. Allison et. al., "A Radiation-Resistant Chromium-Activated Aluminum Oxide Scintillator", UCRL-19270, UC-37 Instruments, TID-4500 (54th Ed.), July 16, 1969.